Journal of Applied Analysis and Computation
Volume 13, Number 2, April 2023, 1044–1069
Website:http://www.jaac-online.com
DOI:10.11948/20220351

MODELING AND ANALYSIS OF LOW-LEVEL TRANSMISSION ZIKV DYNAMICS VIA A POISSON POINT PROCESS ON SEXUAL TRANSMISSION ROUTE

Wenjing Zhang[1,†] and Chathuri T. Sandamali[1]

Abstract In this project, we modeled the low-level ZIKV transmission that was reported in Thailand [31]. The secondary sexual transmission route is modeled by a Poisson point process, which leads to an increasing and saturating contact rate. This nonlinear contact rate further induces backward and Hopf bifurcations. Oscillations bifurcating from the Hopf bifurcation demonstrate the low-level persistent ZIKV transmission with sharp outbreaks, which further show varying amplitudes and frequency by considering stochastic variations on the sexual transmission rate. Global stability analysis of the disease-free equilibrium drives the disease elimination criteria for models considering vector transmission route only and considering both vector and sexual transmission routes. Bifurcation analyses prove the existence of forward and backward bifurcations, saddle-node bifurcation, and Bogdanov-Takens analytically, and further suggest the occurrence of cusp, Hopf, and general Hopf bifurcations numerically. One and two-dimensional bifurcation diagrams demonstrate the analytical results under the influence of both vector and sexual transmission rates. Sensitivity analysis suggests that an increase in mosquito death rate has the largest effect on the basic reproduction number, and an increase in human recovery rate has the most influence on decreasing human host prevalence.

Keywords Low-level ZIKV transmission dynamics, poisson point process, global stability, bifurcation analysis.

MSC(2010) 37N25, 34C20, 34C23, 34C25.

1. Introduction

Zika virus (ZIKV) belongs to the virus family *Flaviviridae* spread by *Aedes* mosquitoes, such as dengue, chikungunya, and yellow fever. The first isolated ZIKV was from the Ziika Forest in Uganda in 1947 [35]. The history of ZIKV outbreaks started in Yap Island in the western Pacific in 2007 [12], leading to the 2013-2014 severe epidemic in French Polynesia [23], before spreading throughout other tropical and subtropic regions in Asia [8], and followed by an explosive epidemic in Latin America in 2015-2016 [18]. Although about one out of five ZIKV infectives develop mild symptoms, including fever, skin rashes, headaches and muscle and/or joint pain [29], with no disease-induced fatalities [13], the infection will results in severe neurological

†The corresponding author. Email: wenjing.zhang@ttu.edu (W. Zhang)
[1]Department of Mathematics and Statistics, Texas Tech University, 1108 Memorial Circle, 79409-1042, Lubbock, TX, USA

complications, such as Guillain-Barré syndrome [7] and congenital microcephaly syndrome in the early stages of pregnancy [26]. Unfortunately, no specific medicine or vaccine exists to treat ZIKV infection.

A sustained low-level ZIKV transmission has been reported for several decades in tropical and subtropic regions from Africa [4,27] to Asia [31] with no reported epidemics. Research evidence shows low-level ZIKV circulations in Thailand for more than 16 years [31] and also in Fiji Islands for several years after the initial introduction [19], and invisible ZIKV endemic challenges in Africa [1, 27]. Even though known the mosquito-to-human spillover, little is heard about the ZIKV transmission patterns because of the misdiagnosis caused by serological cross-reactivity with closely connected dengue virus, the small fraction of symptom cases, and the epidemic burnout due to the high levels of population immunity from the lifelong immunity against reinfection. Due to the close genetic and transmission relation between ZIKV and dengue virus, the same epidemiological, economic, and globalization factors that facilitate the transmission of endemic dengue virus can also be potential threats to the re-emergence of ZIKV in the regions with previous outbreak history. Since approximately 3.6 billion people are infested with *Aedes* mosquitoes, which transmit both dengue and ZIKV viruses, it is necessary to develop sustained prevention and surveillance programs.

Given the potential of ZIKV re-emergence in the endemic dengue region, it is crucial to investigate the low-level sustained ZIKV transmission dynamics. Many mathematical models are proposed to characterize the ZIKV transmission pattern. Most of them are focused on both vector-borne and non-vector-borne transmission routes. As a member of the mosquito-borne family of flaviviruses, ZIKV is still mainly spread by infected *Aedes* mosquitoes' bites. The unique human-human (sexual) transmission is reported to have a much longer duration of infectivity, which might play an important part in introducing ZIKV to non-endemic areas [4]. Saad-Roy et al. [32] proposed a model giving consideration to both vector and sexual transmission routes and distinguishing the sexually inactive and active groups. They concluded that even though sexual transmission could not drive the epidemic alone due to the negligible influence on the basic reproduction number, but it could lead to complex dynamics, such as backward and Hopf bifurcations. Gao et al. [15] considered both transmission routes as well and concluded that the biting and mortality rates of mosquitoes in the vector transmission route had the most significant control on the basic reproduction number, while the sexual transmission route mostly contributed to the increase in the severity of the epidemic. In addition to both transmission routes, Biswas et al. [6] considered mosquito control and public awareness to develop an effective policy for disease control. Taylor [37] recently evaluated various prevention measurements by incorporating both mosquito bite prevention and sexual transmission prevention, and concluded that mosquito bite control strategy has a more significant effect on disease eradication and mitigation than sexual transmission prevention.

No documented disease-induced fatality is another feature of ZIKV transmission. Disease-induced mortality in humans is proposed to be the cause of backward bifurcation [17]. The existence of backward bifurcation not only increases the effort for disease elimination [39], but also leads to complex dynamical behaviors [32]. More specifically, it results that the conventional criterion for disease elimination, that is the reproduction number being below the unity, is no longer adequate [24, 28, 40], and requires more efforts or more effective control strategies. Many mathematical

models considering vector-borne diseases demonstrate backward bifurcations by assuming the existence of disease-induced deaths [2,5]. However, it does not apply to ZIKV transmission.

As a flavivirus, ZIKV triggers a humoral antibody response, which can cross-react with several flavivirus antigens and induces lifelong immunity against reinfection [4]. ZIKV transmission is purposed to burn out the susceptible population, and the disease extinction will follow under sufficiently large population immunity [14]. Nevertheless, Ruchusatsawat et al. [31] pointed out the idea of limited population immunity, which concluded from the similar incidence patterns observed in Thailand and Puerto Rico [11,25]. They further suggested that the current ZIKV transmission is sufficiently high to self-sustain without resulting in large-scale immunity. As a result, the susceptible population pool still exists, but is limited. Due to the insufficiency of the susceptible population, the sexual transmission route experiences a shortage of mating encounters.

Considering the features, we formulate a model to study the low-level persistent ZIKV transmission dynamics. The overview of the paper is as follows. Here, in Section 2, we present the mathematical framework. In Section 3, we analyze the proposed model for the well-posedness, the existence of equilibrium, and their local and global stability. In Section 4, we further carry out the bifurcation analysis, derive the corresponding normal forms, and plot bifurcation diagrams. Simulations for the low-level ZIKV transmission and outbreaks are given in section 5. In Section 6, we discuss disease control strategies through sensitivity analysis. Finally, a conclusion is drawn in Section 7.

2. Model formulation

After the pioneering work by Kermack and McKendrik [21], we categorize the host community into compartments depending on the stage of infection. By assuming no latency period for the disease in human host, the SEIR model framework is reduced to SIR compartmental model. The subscripts h and v represent the human host and mosquito vector populations, respectively. We denote the scaled concentration of the susceptible, infected, and recovered humans as S_h, I_h, and R_h with a rate of recruitment H and a natural mortality rate μ_h, and represent the scaled concentration of infected and susceptible mosquitoes as I_v and S_v with birth and natural death rates of V and μ_v, respectively. Disease-related deaths are not considered due to the rare occurrence. The disease-clearance rate is denoted as γ_h, i.e., the mean time that the virus in blood and semen is $\frac{1}{\gamma_h}$. The two transmission routes are through infected mosquitoes to susceptible humans at the rate of β_{vh}, an infected human to a susceptible mosquito at the rate of β_{hv}, and through direct sexual contact at β. Assuming a homogeneous mixing between human hosts and mosquito vectors, we adopt mass action incidences for the vector-human transmission route. Considering the sparse susceptible human population after an epidemic wave, we consider a heterogeneous mixing among human population to model the shortage of mating encounters. The ZIKV transmission model is written as

$$\begin{aligned}
\frac{dS_h}{dt} &= H - \beta_{hv} S_h I_v - \beta(I_h) I_h S_h - \mu_h S_h, \\
\frac{dI_h}{dt} &= \beta_{hv} S_h I_v + \beta(I_h) I_h S_h - \mu_h I_h - \gamma_h I_h,
\end{aligned}$$

$$\begin{aligned}
&\frac{dR_h}{dt} = \gamma_h I_h - \mu_h R_h,\\
&\frac{dS_v}{dt} = V - \beta_{vh} I_h S_v - \mu_v S_v,\\
&\frac{dI_v}{dt} = \beta_{vh} I_h S_v - \mu_v I_v, \quad \text{where}\\
&\beta(I_h) = \beta_h \frac{I_h}{I_h + K}.
\end{aligned} \tag{2.1}$$

Table 1. Descriptions and values of parameters [16, 32, 36].

Param.	Definition	Value
H	Recruitment rate of human individuals (humans day^{-1})	0.3653×10^{-4}
V	Recruitment rate of vectors (mosquitoes day^{-1})	0.02
μ_h	Natural death rate of human individuals (day^{-1})	0.3653×10^{-4}
μ_v	Natural death rate of vectors (day^{-1})	0.02
β_{hv}	Transmission rate between I_v and S_h (mosquito $^{-1}$ day^{-1})	0.7
β_{vh}	Transmission rate between S_v and I_h (human $^{-1}$ day^{-1})	0.7
β_h	Maximum transmission rate between S_h and I_h (human $^{-1}$ day^{-1})	2
γ_h	Recovery rate of infected humans (day^{-1})	0.01
K	half-saturated level for infected humans	0.3

2.1. Sexual transmission rate derived from pure birth processes

Considering the human population after an epidemic wave, the spread of ZIKV establishes a wide-spread immunity in its human host. As a result, the susceptible human population is sparse. It is assumed that an infected and a susceptible individual are scattered on a real line. We denote the transmission rate as $\beta = \hat{\beta}_h C_E$. Here $\hat{\beta}_h$ is the maximum sexual transmission rate, and C_E is the mating encounter between infected and susceptible humans. Considering the randomness in human mating encounters, we model the infected human's searching distance as a Poisson point process, then consider the mating encounter/probability as a pure birth process. Assuming homogeneous mixing in human hosts, we define the searching distance of a given infected human as a random variable a, an encounter between the infected human and a susceptible human as an event, then the total number of the events is denoted as $Y(a)$, where a is the distance that the infected human search for a susceptible human. Moreover, the number of mating encounters for a positive searching distance is assumed to be a stochastic process $\{Y(a),\, a \geq 0\}$. The following four conditions are satisfied.

1. $Y(0) = 0$, meaning no mating encounters occur if the infected individual has no searching movement.

2. The number of encounters in the interval $(a_1, a_2]$, $Y(a_2) - Y(a_1)$, is independent of the number of encounters in the interval $(a_3, a_4]$, $Y(a_4) - Y(a_3)$, for any $0 \leq a_1 < a_2 \leq a_3 < a_4$. This indicates the Markov property of this process.
3. $Y(a_2 + \Delta a) - Y(a_1 + \Delta a)$ has the same distribution as that of $Y(a_2) - Y(a_1)$, for any $0 \leq a_1 < a_2$, for all $\Delta a > 0$. It indicates stationary increments of this process; that is, the additional number of encounters depends entirely on the searching distance.
4. $\mathbb{P}(Y(a + \Delta a) = 1 | Y(a) = 0) = h(I)\,\Delta a + o(\Delta a)$ and $\mathbb{P}(Y(a + \Delta a) \geq 2 | Y(a) = 0) = o(\Delta a)$, where $\mathbb{P}$ denotes probability. For a new mating encounter per unit distance, we denote the instantaneous transition rate as $h(I_h) = b\dfrac{I_h}{I_h + \tilde{K}}$, where $b > 0$ is the probability of an infected individual per unit of searching length, $\tilde{K}$ is the infected human population density at the disease half-saturating level.

Conditions (1)-(4) indicate the total mating encounters $\{Y(a), a \geq 0\}$ is a Poisson point process. $h(I)$ describes the positive cooperation effect from peer infected humans of interest due to the weaker transmission capability in the secondary transmission route. Since the sexual transmission is secondary to the primary vector-human transmission pathway from mosquitoes to humans, more than one sexual contact may be needed for successful transmission [32]. Therefore, we take $h(I_h)$ as an increasing and saturating function in the form. By conditions (1)-(4), $\{Y(a)\}_{a \geq 0}$ is a simple birth-death process. It follows that

$$p_0(a) = \mathbb{P}\{Y(a) = i\} = \mathbb{P}\{Y(a) = 0 | Y(0) = 0\} = e^{-ah(I_h)}. \tag{2.2}$$

Moreover, we only consider the successful sexual transmission encounter and treat multiple sexual encounter as part of a successful encounter. Therefore, we only consider the probability of no encounter and the probability of at least one encounter, which are given as

$$\mathbb{P}\{Y(a) = 0\} = p_0(a) = e^{-ah(I_h)}, \quad \mathbb{P}\{Y(a) \geq 1\} = 1 - p_0(a) = 1 - e^{-ah(I_h)}. \tag{2.3}$$

Therefore, the mating encounter C_E is the expectation of the encounter event occurring at least one time with respect to a searching length a, which is assumed as an exponential distribution with parameter $\alpha_1 > 0$. That is

$$C_E = \mathbb{E}\left[1 - p_0(a)\right] = 1 - \mathbb{E}\left[p_0(a)\right] = \frac{h(I_h)}{\alpha_1 + h(I_h)} = \frac{b}{b + \alpha_1}\frac{I_h}{I_h + K}, \tag{2.4}$$

where $K = \frac{\alpha_1 \tilde{K}}{b + \alpha_1 \tilde{K}}$ and $\mathbb{E}$ denotes the expectation. The sexual transmission rate β is a function of infected human hosts I_h, such that $\beta(I_h) = \beta_h \frac{I_h}{I_h + K}$, where $\beta_h = \hat{\beta}_h \frac{b}{b + \alpha_1}$.

3. Model analysis

3.1. Positiveness and boundedness of the solutions

Theorem 3.1. *Given non-negative initial conditions, solutions of model* (2.1) *remain non-negative for all* $t \geq 0$. *Moreover, the biologically feasible region* Γ *is*

positively invariant and globally attracting, where

$$\Gamma = \left\{ (S_h, I_h, R_h, S_v, R_v) \in \mathbb{R}^5_+ | 0 < S_h + I_h + R_h = \frac{H}{\mu_h}, 0 < S_v + I_v = \frac{V}{\mu_v} \right\}. \tag{3.1}$$

Proof. First, we derive the total population densities for human and vector as

$$N_h(t) = S_h(t) + I_h(t) + R_h(t), \qquad N_v(t) = S_v(t) + I_v(t),$$

which are governed by

$$\frac{dN_h(t)}{dt} = H - \mu_h N_h(t), \qquad \frac{dN_v(t)}{dt} = V - \mu_v N_v(t).$$

We notice that $N_h(t)$ and $N_v(t)$ approach constants asymptotically in forward time as

$$\lim_{t\to\infty} N_h(t) = \frac{H}{\mu_h}, \qquad \lim_{t\to\infty} N_v(t) = \frac{V}{\mu_v}.$$

Next, we consider initial conditions in the bounded region, Γ, and study the direction of the vector field of the model (2.1) on the boundary of $\mathbb{R}^5_+$. We derive

$$\frac{dS_h}{dt}|_{S_h=0} = H \geq 0, \ \frac{dI_h}{dt}|_{I_h=0} = \beta_{hv} S_h I_v \geq 0, \ \frac{dR_h}{dt}|_{R_h=0} = \gamma_h I_h \geq 0,$$
$$\frac{dS_v}{dt}|_{S_v=0} = V \geq 0, \ \frac{dI_v}{dt}|_{I_v=0} = \beta_{vh} I_h S_v \geq 0.$$

The vector field of model (2.1) on the boundary of $\mathbb{R}^5_+$ is either tangential to the boundary or pointing to its interior. It follows that the bounded region Γ is positively invariant. Moreover, the inequalities $\frac{dI_h}{dt} > 0$ and $\frac{dI_v}{dt} > 0$ imply that the existence of infected mosquitoes and/or infected humans in the environment is a possible cause to trigger a disease outbreak. □

3.2. The basic reproduction number

The invading ability of an infectious disease is measured by its basic reproduction number. We apply the method of next-generation matrix [39] and obtain the spectral radius $\rho(\cdot)$ of FV^{-1} as follows,

$$R_0 = \rho(FV^{-1}) = \rho\left(\begin{bmatrix} 0 & \frac{\beta_{hv} H}{\mu_h} \\ \frac{\beta_{vh} V}{\mu_v} & 0 \end{bmatrix} \begin{bmatrix} \mu_h + \gamma_h & 0 \\ 0 & \mu_v \end{bmatrix}^{-1} \right) = \sqrt{\frac{\beta_{hv}\beta_{vh} HV}{\mu_h {\mu_v}^2 (\mu_h + \gamma_h)}}. \tag{3.2}$$

The threshold value $R_0(\beta_{hv}) = 1$ is equivalent to

$$\beta_{hv} = \frac{\mu_h {\mu_v}^2 (\mu_h + \gamma_h)}{\beta_{vh} HV} \triangleq \hat{\beta}_{hv}. \tag{3.3}$$

3.3. Equilibrium solutions

Setting $\frac{dS_h}{dt} = \frac{dI_h}{dt} = \frac{dR_h}{dt} = \frac{dS_v}{dt} = \frac{dI_v}{dt} = 0$ yields

$$\begin{aligned} S_h^* &= \frac{H(K + I_h^*)}{\beta_h I_h^{*2} + (\beta_{hv} I_v^* + \mu_h)(K + I_h^*)}, \\ R_h^* &= \frac{\gamma_h I_h^*}{\mu_h}, \\ S_v^* &= \frac{V}{\beta_{vh} I_h^* + \mu_v}, \\ I_v^* &= \frac{\beta_{vh} V I_h^*}{\mu_v(\beta_{vh} I_h^* + \mu_v)}, \end{aligned}$$

where I_h^* is the root of the cubic equation

$$\begin{aligned} & I_h(a_3 {I_h}^3 + a_2 {I_h}^2 + a_1 I_h + a_0) = 0, \\ & a_3 = \beta_{vh}\beta_h\mu_v M_1 > 0, \\ & a_2 = \beta_{vh} M_1 M_2 + \mu_v^2 \beta_h M_1 - H\beta_h\mu_v\beta_{vh}, \\ & a_1 = \mu_h\mu_v M_1(1 - R_0^2) + K\beta_{vh} M_1 M_2 - H\beta_h\mu_v^2, \\ & a_0 = K\mu_h\mu_v^2 M_1(1 - R_0^2), \\ \text{where} \quad & M_1 = \mu_h + \gamma_h,\ M_2 = V\beta_{hv} + \mu_h\mu_v. \end{aligned} \tag{3.4}$$

The preceding equation admits an endemic equilibrium $E^* = (S_h^*, I_h^*, R_h^*, S_v^*, I_v^*)$ and a trivial solution $I_h = 0$. We, then, derive the following theorem.

Theorem 3.2. *Model* (2.1) *always admits a disease-free equilibrium,*

$$E_0 = \left(\frac{H}{\mu_h}, 0, 0, \frac{V}{\mu_v}, 0\right).$$

3.4. Local stability of the disease-free equilibrium

To further investigate the dynamical behaviors of the model (2.1) under the influence of sexual and host-vector transmissions, we investigate the local stability of the disease-free equilibrium.

Theorem 3.3. *If $R_0 < 1$, E_0 is locally asymptotically stable in Γ. If $R_0 > 1$, E_0 becomes a saddle and is unstable.*

Proof. The Jacobian matrix is derived for the model (2.1) at E_0 as follows,

$$J|_{E_0} = \begin{bmatrix} -\mu_h & 0 & 0 & 0 & -\dfrac{\beta_{hv}H}{\mu_h} \\ 0 & -\mu_h - g & 0 & 0 & \dfrac{\beta_{hv}H}{\mu_h} \\ 0 & \gamma_h & -\mu_h & 0 & 0 \\ 0 & -\dfrac{\beta_{vh}V}{\mu_v} & 0 & -\mu_v & 0 \\ 0 & \dfrac{\beta_{vh}V}{\mu_v} & 0 & 0 & -\mu_v \end{bmatrix}, \tag{3.5}$$

which admits three negative eigenvalue as $\lambda_{1,2,3} = -\mu_h, -\mu_h, -\mu_v < 0$. The other two eigenvalues λ_4 and λ_5 are determined by the following quadratic equation,

$$\lambda^2 + (\mu_h^2\mu_v + \mu_v^2\mu_h + \mu_h\mu_v\gamma_h)\lambda + {\mu_h}^2{\mu_v}^2 + \mu_h\mu_v^2\gamma_h - HV\beta_{hv}\beta_{vh} = 0.$$

Notice that

$$\lambda_4 + \lambda_5 = -(\mu_h^2\mu_v + \mu_v^2\mu_h + \mu_h\mu_v\gamma_h) < 0,$$

$$\lambda_4\lambda_5 = {\mu_h}^2{\mu_v}^2 + \mu_h\mu_v^2\gamma_h - HV\beta_{hv}\beta_{vh} = \frac{1}{\mu_h\mu_v^2(\mu_h + \gamma_h)}(1 - R_0^2).$$

We have $\lambda_4\lambda_5 > 0$ if $R_0 < 1$, and thus both λ_4 and λ_5 are either negative real numbers or complex conjugates having negative real parts. In this case, E_0 shows asymptotic stability. If $R_0 > 1$, we have $\lambda_4\lambda_5 < 0$, and then λ_4 and λ_5 have opposite signs. Hence, E_0 is unstable. □

3.5. The global stability of E_0 without human-human sexual transmission route

Noticing that R_0 in (3.2) depends only on β_{hv}, which represents the vector-human transmission rate, but is independent of β_h, which represents the human-human transmission route, we, therefore, first consider only the host-vector transmission route and obtain the following results.

Theorem 3.4. *In the absence of the human-human sexual transmission route, that is $\beta_h = 0$, the disease-free equilibrium, E_0 is globally asymptotically stable if $R_0 < 1$, and is uniformly persistent if $R_0 > 1$.*

Proof. Consider the model (2.1) with no sexual transmission ($\beta_h = 0$), we group the disease and non-disease compartments as

$$X = (I_h, I_v)^T \in \mathbb{R}^2 \quad \text{and} \quad Y = (S_h, R_h, S_v)^T \in \mathbb{R}^3.$$

Based on the Theorems 2.1 and 2.2 in [34], we derive a Lyapunov function for the model (2.1) as $Q = vV^{-1}X$, where

$$v = \left[\sqrt{\frac{(\mu_h + \gamma_h)\mu_h\beta_{vh}V}{\beta_{hv}H\mu_v^2}},\ 1\right]$$

and V^{-1} in equation (3.2). Calculation yields

$$Q = \frac{I_h}{\mu_h + \gamma_h}\sqrt{\frac{(\mu_h + \gamma_h)\mu_h\beta_{vh}V}{\beta_{hv}H\mu_v^2}} + \frac{I_v}{\mu_v}.$$

It follows

$$\begin{aligned}
\frac{dQ}{dt} &= \sqrt{\frac{\mu_h\beta_{vh}V}{\beta_{hv}H\mu_v^2(\mu_h+\gamma_h)}}\,(\beta_{hv}S_hI_v - \mu_hI_h - \gamma_hI_h) + \frac{\beta_{vh}I_hS_v - \mu_vI_v}{\mu_v} \\
&\le \sqrt{\frac{(\mu_h+\gamma_h)\mu_h\beta_{vh}V}{\beta_{hv}H\mu_v^2}}\left(-I_h + \frac{\beta_{hv}HI_v}{\mu_h(\mu_h+\gamma_h)}\right) + \frac{\beta_{vh}VI_h}{\mu_v^2} - I_v \\
&= \left(\sqrt{\frac{(\mu_h+\gamma_h)\mu_h\beta_{vh}V}{\beta_{hv}H\mu_v^2}}I_h + I_v\right)\left(\sqrt{\frac{\beta_{vh}V\beta_{hv}H}{\mu_h\mu_v^2(\mu_h+\gamma_h)}} - 1\right) \\
&= \left(\sqrt{\frac{(\mu_h+\gamma_h)\mu_h\beta_{vh}V}{\beta_{hv}H\mu_v^2}}I_h + I_v\right)(R_0 - 1) \le 0.
\end{aligned}$$

Since the disease-free equilibrium shows local stability, the only invariant set is E_0 in $\mathbb{R}^5_+$, where $X = 0 \in \mathbb{R}^2$. Moreover, $\frac{dQ}{dt} \equiv 0$ when $X = 0$. Then, LaSalle's invariance principle provides that E_0 is globally asymptotically stable if $R_0 < 1$. Following the Theorem 2.2 in [34], if $R_0 > 1$ the disease-free equilibrium E_0 becomes unstable and the system (2.1) with $\beta_h = 0$ is uniformly persistent. The system exhibits at least one endemic equilibrium given the infection is initially present. □

3.6. Global stability of E_0 under host-vector and host-host transmission routes

Considering both transmission routes, we derive a new disease elimination threshold R_1 in the following theorem.

Theorem 3.5. *Disease elimination can be achieved, that is, the infection-free equilibrium E_0 is globally asymptotically stable if $R_0 < R_1 < 1$ where $R_1^2 = R_0^2 + \dfrac{\beta_h H^2}{\mu_h^2 K(\gamma_h + \mu_h)}$.*

Proof. Applying the fluctuation lemma [38], we first consider the positive and bounded function $x : (0, \infty) \to \mathbb{R}$ and denote $x^\infty = \limsup_{t\to\infty} x(t)$ and $x_\infty = \liminf_{t\to\infty} x(t)$. According to the fluctuation lemma, sequences $\{s_n\}$ and $\{\tau_n\}$ exist such that as $s_n \to \infty$ and $\tau_n \to \infty$, solutions of model (2.1) satisfy $\lim_{n\to\infty} x_i(s_n) = x_{i\infty}$, $\lim_{n\to\infty} \dot{x_i}(s_n) = 0$, $\lim_{n\to\infty} x_i(\tau_n) = x_i^\infty$, and $\lim_{n\to\infty} \dot{x_i}(\tau_n) = 0$, for all $x_i(t)$, $i = 1..5$. Corresponding the first and fourth equations in (2.1), we have

$$\begin{aligned}
&\dot{x_1}(\tau_n) + \beta_{hv}x_1(\tau_n)x_5(s_n) + \beta_h\frac{(x_2(s_n))^2}{K + x_2(s_n)}x_1(\tau_n) + \mu_hx_1(\tau_n) = H, \\
&\dot{x}_4(\tau_n) + \beta_{vh}x_2(s_n)x_4(\tau_n) + \mu_vx_4(\tau_n) = V.
\end{aligned}$$

As $n \to \infty$, with the non-negative properties of the solutions $x_i(t)$, for $i = 1 \dots 5$,

we have

$$\mu_h x_1^\infty \le \beta_{hv} x_1^\infty x_5^\infty + \beta_h \frac{(x_{2\infty})^2}{K + x_{2\infty}} x_1^\infty + \mu_h x_1^\infty \le H,$$
$$\mu_v x_4^\infty \le \beta_{vh} x_{2\infty} x_4^\infty + \mu_v x_4^\infty \le V.$$

It follows $x_1^\infty \le \frac{H}{\mu_h}$ and $x_4^\infty \le \frac{V}{\mu_v}$. Applying the fluctuation lemma on the second and fifth equations in model (2.1) again, we have

$$\begin{aligned}
&(\gamma_h + \mu_h) x_2^\infty \le \beta_{hv} x_1^\infty x_5^\infty + \beta_h \frac{x_2}{K + x_2} x_2^\infty x_1^\infty \le \frac{\beta_{hv} H}{\mu_h} x_5^\infty + \frac{\beta_h H}{\mu_h} \frac{x_2}{K + x_2} x_2^\infty, \\
&\mu_v x_5^\infty \le \beta_{vh} x_2^\infty x_4^\infty \le \frac{\beta_{vh} V}{\mu_v} x_2^\infty.
\end{aligned} \tag{3.6}$$

Also, noticing that

$$\frac{x_2}{K + x_2} \le \frac{x_2^\infty}{K} \quad \text{for} \quad x_2^\infty \ge 0 \tag{3.7}$$

in the bounded region Γ shown in (3.1), we have

$$x_2 \le x_1^\infty + x_2^\infty + x_3^\infty \le \frac{H}{\mu_h}, \tag{3.8}$$

thus

$$\frac{x_2}{K + x_2} \le \frac{x_2^\infty}{K} \le \frac{H}{\mu_h K}. \tag{3.9}$$

By combining the preceding inequalities with (3.6), we get

$$(\gamma_h + \mu_h) x_2^\infty \le \frac{\beta_{hv} \beta_{vh} H V}{\mu_h \mu_v^2} x_2^\infty + \frac{\beta_h H^2}{\mu_h^2 K} x_2^\infty, \tag{3.10}$$

which is equivalent to

$$x_2^\infty \left(\gamma_h + \mu_h\right) \left[1 - \tilde{R}_1^2(x_2^\infty)\right] \le 0 \tag{3.11}$$

with

$$R_1^2 = \tilde{R}_1^2(x_2^\infty) = R_0^2 + \frac{\beta_h H^2}{\mu_h^2 K(\gamma_h + \mu_h)}. \tag{3.12}$$

When $R_0 < R_1 < 1$, we have $x_2^\infty = 0$ followed by $x_2^\infty \ge 0$. It yields $x_3^\infty = 0$ and $x_5^\infty = 0$. Due to the non-negativity of the solutions in Theorem 3.1, we have $0 \le x_{2\infty} \le x_2^\infty = 0$, which yields $\lim_{t \to +\infty} x_2(t) = 0$. It follows $\lim_{t \to +\infty} x_3(t) = 0$ and $\lim_{t \to +\infty} x_5(t) = 0$. Then the limiting equation for x_1 and x_4 are $\dot{x}_1 = H - \mu_h x_1$ and $\dot{x}_4 = V - \mu_v x_4$. Thus we have $\lim_{t \to +\infty} x_1(t) = \frac{H}{\mu_h}$ and $\lim_{t \to +\infty} x_4(t) = \frac{V}{\mu_v}$. □

3.7. The threshold for the disease elimination with one imported infected human

The preceding subsection derives the sufficient condition for disease elimination, that is $R_0 < R_1 < 1$. This condition can be relaxed at the initiation of the epidemics, when the imported infected human population is tiny. To get a more intuitive understanding of the epidemic dynamics at the initiation stage, we derive the

threshold for disease elimination from the first principle. Let us start with one imported infected human and assume all humans are susceptible. Then the expected number of infected mosquitoes and infected human from this primary imported infected human are:

$$\begin{aligned}&\text{infected mosquitoes} = \beta_{vh}\,\frac{V}{\mu_v}\,\frac{1}{\mu_h+\gamma_h} \quad \text{and}\\ &\text{infected humans via sexual tranmission} = \beta_h\,\frac{1}{1+K}\,\frac{H}{\mu_h}\,\frac{1}{\mu_h+\gamma_h}.\end{aligned} \tag{3.13}$$

Then, we derive the number of humans infected by this newly infected mosquito as follows:

$$\text{infected humans via vector tranmission} = \beta_{hv}\,\frac{H}{\mu_h}\,\frac{1}{\mu_v}. \tag{3.14}$$

Thus, the number of secondary infections in human hosts from the primary imported infected human host is

$$\begin{aligned}\text{secondary infected humans} &= \beta_{vh}\,\frac{V}{\mu_v}\,\frac{1}{\mu_h+\gamma_h}\,\beta_{hv}\,\frac{H}{\mu_h}\,\frac{1}{\mu_V}+\beta_h\,\frac{1}{1+K}\,\frac{H}{\mu_h}\,\frac{1}{\mu_h+\gamma_h}\\ &= R_0^2+\frac{\beta_h\,H}{\mu_h\,(1+K)\,(\mu_h+\gamma_h)} = \tilde{R}_1^2(x_2=1).\end{aligned} \tag{3.15}$$

Denoting $\tilde{R}_1^2(x_2=1)=R_{11}$, we conclude that disease elimination can be achieved with one imported infected human if we can bring the basic reproduction number under R_{11}, that is $R_0 < R_{11} < 1$.

4. Bifurcation analysis

In order to achieve a better understanding of the ZIKA transmission under both vector-human and human-human tranmission routes, we carry out bifurcation analysis. First, we rewrite the model in a general form as

$$\frac{dx}{dt} = f(x,\,\phi), \tag{4.1}$$

where

$$x = (x_1,x_2,x_3,x_4,x_5)^T = (S_h,I_h,R_h,S_v,I_v)^T \qquad \text{and}$$

$$f = (f_1,f_2,f_3,f_4,f_5)^T = \left(\frac{dS_h}{dt},\frac{dI_h}{dt},\frac{dR_h}{dt},\frac{dS_v}{dt},\frac{dI_v}{dt}\right)^T.$$

We denote all positive parameters in model (2.1) as $\phi = (\phi_f,\,\phi_b)$, where ϕ_f are fixed parameters and ϕ_b bifurcation parameters. In this project, we choose β_h and β_{hv} as potential bifurcation parameters, and fix the other parameters as their baseline values in Table 1.

4.1. Forward and backward bifurcations

Forward and backward bifurcation occur by varying both the vector-host and host-host transmission rates. For the case $R_0 = 1$ or $\beta_{hv} = \hat{\beta}_{hv}$ in (3.3), we study the

disease-free equilibrium E_0 on its center manifold. In this case, ϕ_b denotes β_{hv}, while ϕ_f represents the rest of the parameters. We denote the Jacobian matrix evaluated at E_0 and $R_0 = 1$ as $D_x f(E_0, \hat{\beta}_{hv}) = J|_{E_0}(\beta_{hv} = \hat{\beta}_{hv})$, which admits four negative eigenvalues and one zero eigenvalue as follows:

$$-\mu_v, \quad -(\mu_h + \mu_v + \gamma_h), \quad -\mu_h, \quad -\mu_h, \quad \text{and} \quad 0.$$

According to [39], we choose the right and left eigenvectors of $D_x f(E_0, \hat{\beta}_{hv})$ resulted by the single zero eigenvalue as follows:

$$\begin{aligned} w &= \left(\frac{-\mu_v^2(\gamma_h + \mu_h)}{\beta_{vh} V \mu_h}, \frac{\mu_v^2}{\beta_{vh} V}, \frac{\mu_v^2 \gamma_h}{\beta_{vh} V \mu_h}, -1, 1 \right)^T, \\ v &= \left(0, \frac{V \beta_{vh}}{\mu_v(\mu_v + \gamma_h + \mu_h)}, 0, 0, \frac{(\gamma_h + \mu_h)}{(\mu_v + \gamma_h + \mu_h)} \right), \end{aligned} \tag{4.2}$$

which satisfy $< v, w >= 1$. Carrying out the shifting transformation as $c(t) = x(t) - E_0$ and $\mu = \beta_{hv} - \hat{\beta}_{hv}$, the center manifold of the infection-free equilibrium at $R_0 = 1$ (or $\beta_{hv} = \hat{\beta}_{hv}$) is denoted by $c(t)$ with its governing differential equation

$$\frac{dc}{dt} = \frac{1}{2}\tilde{a}c^2 + \tilde{b}\mu c. \tag{4.3}$$

The coefficient $\tilde{a}$ and $\tilde{b}$ are

$$\tilde{a} = \sum_{i,j,k=1}^{5} v_i w_j w_k \frac{\partial^2 f_i}{\partial x_j \partial x_k}(E_0, \hat{\beta}_{hv}), \quad \tilde{b} = \sum_{i,k=1}^{5} v_k w_i \frac{\partial^2 f_k}{\partial x_i \partial \mu}(E_0, \hat{\beta}_{hv}),$$

where $w = (w_1, w_2, w_3, w_4, w_5)^T$ and $v = (v_1, v_2, v_3, v_4, v_5)$ are chosen as in (4.2). The nonzero coefficients are

$$\frac{\partial^2 f_1}{\partial x_1 \partial x_5}|_{(0,0)} = \frac{\partial^2 f_1}{\partial x_2 \partial x_1}|_{(0,0)} = \frac{-\partial^2 f_2}{\partial x_1 \partial x_5}|_{(0,0)} = \frac{-\partial^2 f_2}{\partial x_5 \partial x_1}|_{(0,0)} = \frac{-\mu_h {\mu_v}^2 (\mu_h + \gamma_h)}{HV\beta_{vh}},$$

$$\frac{\partial^2 f_2}{\partial {x_2}^2}|_{(0,0)} = -\frac{\partial^2 f_1}{\partial {x_2}^2}|_{(0,0)} = \frac{2\beta_h H}{K\mu_h},$$

$$\frac{\partial^2 f_5}{\partial x_2 \partial x_4}|_{(0,0)} = \frac{\partial^2 f_5}{\partial x_4 \partial x_2}|_{(0,0)} = -\frac{\partial^2 f_4}{\partial x_2 \partial x_4}|_{(0,0)} = -\frac{\partial^2 f_4}{\partial x_4 \partial x_2}|_{(0,0)} = \beta v h,$$

$$\frac{\partial^2 f_2}{\partial x_5 \partial \mu}|_{(0,0)} = -\frac{\partial^2 f_1}{\partial x_5 \partial \mu}|_{(0,0)} = \frac{H}{\mu_h}.$$

It follows

$$\begin{aligned} \tilde{a} &= \frac{2\mu_v^2(-K\mu_v\mu_h^3 - K(H\beta_{vh} + 2\gamma_h\mu_v)\mu_h^2 - K\gamma_h(H\beta_{vh} + \gamma_h\mu_v)\mu_h + H^2\beta_h\mu_v)}{\mu_h\ (\mu_v + \mu_h + \gamma_h)\, KV\beta_{vh}}, \\ \tilde{b} &= \frac{HV\beta_{vh}}{(\mu_v + \mu_h + \gamma_h)\,\mu_v\,\mu_h} > 0. \end{aligned} \tag{4.4}$$

Since the coefficient b is positive for all parameter values which are considered to be positive. We derive the following result.

Theorem 4.1. *The infection-free equilibrium E_0 of the ZIKV model* (2.1) *undergoes a transcritical bifurcation at $R_0 = 1$ (or $\beta_{hv} = \hat{\beta}_{hv}$), which presents a forward (backward) bifurcation if $\tilde{a} < 0\,(> 0)$. Moreover, $\tilde{a} < 0$ is equivalent to*

$$\beta_h < \hat{\beta}_h = \frac{\mu_h K (\gamma_h + \mu_h)(H\beta_{vh} + (\gamma_h + \mu_h)\mu_v)}{\mu_v H^2}.$$

Examples for forward and backward bifurcations. We choose β_{hv} as the bifurcation parameter, take two parameter values for β_h, and set the other parameter values constant as given in Table 1. When $\beta_h = 0.2$, the coefficients for the center manifold in (4.3) near E_0 at $\beta_{hv} = 0.00028676$ are $\tilde{a} = -0.092920$ and $\tilde{b} = 23.305$, which implies a forward bifurcation. When $\beta_h = 3$, these coefficients are $\tilde{a} = 0.26220$ and $\tilde{b} = 23.305$, which implies a backward bifurcation. The corresponding bifurcation diagrams are shown in Figure 2.

4.2. Saddle-node bifurcation

Saddle-node bifurcation occurs on endemic equilibrium $E^* = (x_1^*, x_2^*, x_3^*, x_4^*, x_5^*)$ when its corresponding Jacobian matrix is

$$J_{E^*} = \begin{bmatrix} -\beta^* x_2^* - \beta_{hv} x_5^* - \mu_h & -\beta^*(2 - \frac{\beta^*}{\beta_h})x_1^* & 0 & 0 & -\beta_{hv} x_1^* \\ \beta^* x_2^* + \beta_{hv} x_5^* & \beta^*(2 - \frac{\beta^*}{\beta_h})x_1^* - \gamma_h - \mu_h & 0 & 0 & \beta_{hv} x_1^* \\ 0 & \gamma_h & -\mu_h & 0 & 0 \\ 0 & -\beta_{vh} x_4^* & 0 & -\beta_{vh} x_2^* - \mu_v & 0 \\ 0 & \beta_{vh} x_4^* & 0 & \beta_{vh} x_2^* & -\mu_v \end{bmatrix} \tag{4.5}$$

where $\beta^* = \beta_h \dfrac{x_2^*}{x_2^* + K}$ and J_{E^*} admits a single zero eigenvalue at

$$\begin{aligned} \beta_{hv} = \beta_{hv}^{SN} := -[&\beta_h(\gamma_h + \mu_h)x_2^{*3} + (\mu_h^2 + (K\beta_h - \beta_h x_1^* + \gamma_h)\mu_h + K\gamma_h\beta_h)x_2^{*2} \\ &+2\mu_h K(-\beta_h x_1^* + \gamma_h + \mu_h)x_2^* + K^2\mu_h(\gamma_h + \mu_h)] \\ &\times \frac{\beta_{vh} x_2^* + \mu_v}{(x_2^* + K)^2[x_5^*\beta_{vh}(\gamma_h + \mu_h)x_2^* + (-\beta_{vh} x_1^* x_4^* + \mu_v x_5^*)\mu_h + \gamma_h x_5^* \mu_v]}. \end{aligned} \tag{4.6}$$

We take an eigenvector associated with the zero eigenvalue and its adjoint eigen-

vector as follows:

$$q=\begin{bmatrix} q_1 \\ 1 \\ \dfrac{\gamma_h}{\mu_h} \\ -\dfrac{\beta_{vh}x_4^*}{\beta_{vh}x_2^*+\mu_v} \\ \dfrac{\beta_{vh}x_4^*}{\beta_{vh}x_2^*+\mu_v} \end{bmatrix}, \quad p=\begin{bmatrix} \dfrac{1}{n_1} \\ \dfrac{\beta_h x_2^{*2}+(\beta_{hv}x_5^*+\mu_h)x_2^*+K(\beta_{hv}x_5^*+\mu_h)}{n_1(K\beta_{hv}x_5^*+\beta_{hv}x_2^*x_5^*+\beta_h x_2^{*2})} \\ 0 \\ \dfrac{\beta_{vh}x_2^*\beta_{hv}x_1^*\mu_h(x_2^*+K)}{n_1\ mu_v(\beta_{vh}x_2^*+\mu_v)(K\beta_{hv}x_5^*+\beta_{hv}x_2^*x_5^*+\beta_h x_2^{*2})} \\ \dfrac{\beta_{hv}x_1^*\mu_h(x_2^*+K)}{n_1\mu_v(\beta_h x_2^{*2}+\beta_{hv}x_5^*(x_2^*+K))}), \end{bmatrix} \tag{4.7}$$

where

$$\begin{aligned} q_1 =& \frac{-x_1^*}{(\beta_{vh}x_2^*+\mu_v)(x_2^*+K)(\beta_h x_2^{*2}+(\beta_{hv}x_5^*+\mu_h)x_2^*+K(\beta_{hv}x_5^*+\mu_h))} \\ & \times[\beta_{vh}\beta_h x_2^{*3}+(2K\beta_{vh}\beta_h+\beta_{hv}\beta_{vh}x_4^*+\beta_h\mu_v)x_2^{*2}+2K(\beta_{hv}\beta_{vh}x_4^*+\beta_h\mu_v)x_2^* \\ & +K^2\beta_{hv}\beta_{vh}x_4^*] \\ n_1 =& q_1-\frac{\beta_{vh}^2 x_2^*\beta_{hv}x_1^*\mu_h x_4^*(x_2^*+K)}{(K\beta_{hv}x_5^*+\beta_{hv}x_2^*x_5^*+\beta_h x_2^{*2})\mu_v(\beta_{vh}x_2^*+\mu_v)^2} \\ & +\frac{\beta_{hv}x_1^*\mu_h\beta_{vh}x_4^*(x_2^*+K)}{\mu_v(\beta_h x_2^{*2}+\beta_{hv}x_5^*(x_2^*+K))(\beta_{vh}x_2^*+\mu_v)} \\ & +\frac{\beta_h x_2^{*2}+(\beta_{hv}x_5^*+\mu_h)x_2^*+K(\beta_{hv}x_5^*+\mu_h)}{K\beta_{hv}x_5^*+\beta_{hv}x_2^*x_5^*+\beta_h x_2^{*2}}. \end{aligned}$$

Carrying out the shifting transformation as $u(t)=x(t)-E_{SN}^*$ and $\mu=\beta_{hv}-\beta_{hv}^{SN}$, the center manifold near $u=0$ and $\mu=0$ takes the form

$$\begin{aligned} & \frac{du}{dt}=b\,u^2+O(u^3), \\ \text{where} \quad & b=\frac{1}{2}\sum_{i,j,k=1}^{5}p_i q_j q_k\frac{\partial^2 f_i(E_{SN}^*,\beta_{hv}^{SN})}{\partial x_j\partial x_k} \\ & =\frac{1}{(x_2^*+K)^3}\{[(p_2-1)(\beta_{hv}q_5+\beta_h)q_1-\beta_{vh}q_4(p_4-p_5)]x_2^{*3} \\ & +3[(p_2-1)(\beta_{hv}q_5+\beta_h)q_1-\beta_{vh}q_4(p_4-p_5)]Kx_2^{*2} \\ & +3[(\beta_{hv}q_5+2/3\beta_h)(p_2-1)q_1-\beta_{vh}q_4(p_4-p_5)]K^2x_2^* \\ & +[(\beta_{hv}q_5(p_2-1)q_1-\beta_{vh}q_4(p_4-p_5))K+\beta_h x_1^*(p_2-1)]K^2\}. \end{aligned} \tag{4.8}$$

Moreover, the transversality condition

$$\sum_{i,\,j=1}^{5}p_j\frac{\partial f_i(E_{SN}^*,\beta_{hv}^{SN})}{\partial\beta_{hv}}=x_5^*x_1^*(p_2-1)\neq 0$$

is satisfied. Here, q_i and p_i are components in the vectors q and p in (4.6). We arrive at the following conclusion.

Theorem 4.2. *The endemic equilibrium E^* of the ZIKV model* (2.1) *admits a single zero eigenvalue at $\beta_{hv} = \beta_{hv}^{SN}$, and is locally topologically equivalent near the origin to*

$$\dot{u} = \mu + b\,u^2,$$

where μ is the small perturbation and the expression of b is shown in (4.8).

Example for saddle-node bifurcation. We choose β_{hv} as the bifurcation parameter, take two parameter values for β_h, and set the other parameter values according to Table 1. Consider that $\beta_h = 0.2$, there exists no saddle-node bifurcation in the biologically feasible region. When $\beta_h = 3$, the endemic equilibrium undergoes a saddle-node bifurcation at the equilibrium point $E_{SN}^* = (0.52982,\ 0.0017113,\ 0.46847,\ 0.94349,\ 0.056511)$ and $\beta_{hv}^{SN} = 0.000058361$. The four corresponding nonzero eigenvalues are -0.021883, -0.02, -0.00003653, and 0.0085594. We take an eigenvector corresponding to the zero eigenvalue $q = (1.0099,\ 0.0036891,\ -1.0136,\ -0.11494,\ 0.11494)^T$ and its associated adjoint eigenvector $p = (0.9824, 2.0894,\ 0,\ 0.0000967,\ 0.0017)$. The coefficient b in the normal form (4.8) is $b = -0.00043119$. The transversality condition $\sum_{i,\,j=1}^{5} p_j \frac{\partial f_i(E_{SN}^*, \beta_{hv}^{SN})}{\partial \beta_{hv}} = -0.063329 \neq 0$ is satisfied. The corresponding bifurcation diagrams are shown in Figure 2.

4.3. Bogdanov-Takens bifurcation (BT)

The endemic equilibrium E^* undergoes a BT bifurcation when the corresponding Jacobian matrix J in (4.5) has double-zero eigenvalues at $(\beta_{hv},\ \beta_h) = (\beta_{hv}^{bt},\ \beta_h^{bt})$ as follows:

$$\begin{aligned}
\beta_{hv}^{bt} =& \frac{1}{(x_2^*+K)^2(\beta_{vh}x_2^*x_5^* + x_5^*\mu_h - x_4^*x_1^*\beta_{vh} + x_5^*(\gamma_h+\mu_v))}\{-\beta_{vh}\beta_h x_2^{*4} \\
&+ [-K\beta_h\beta_{vh} + (-2\beta_{vh}-\beta_h)\mu_h + (\beta_{vh}x_1^* - \gamma_h - \mu_v)\beta_h - \gamma_h\beta_{vh}]x_2^{*3} \\
&+ (((-4\beta_{vh}-\beta_h)\mu_h + (2\beta_{vh}x_1^* - \gamma_h - \mu_v)\beta_h - 2\gamma_h\beta_{vh})K - \mu_h^2 \\
&+ (\beta_h x_1^* - \gamma_h - 2\mu_v)\mu_h - \mu_v(-\beta_h x_1^* + \gamma_h))x_2^{*2} - (\beta_{vh}(\gamma_h + 2\mu_h)K \\
&+ 2\mu_h^2 + (-2\beta_h x_1^* + 2\gamma_h + 4\mu_v)\mu_h + 2\mu_v(-\beta_h x_1^* + \gamma_h))Kx_2^* \\
&- (\mu_h^2 + (\gamma_h + 2\mu_v)\mu_h + \gamma_h\mu_v)K^2\}, \\
\beta_h =& \frac{1}{2x_1^*x_2^*\beta_{hn}}(x_2^*+K)^2[x_2^*(-x_5^*(\gamma_h+\mu_h)^2x_2^* + \mu_h^2x_1^*x_4^*)\beta_{vh}^2 \\
&+ (-2x_5^*\mu_v(\gamma_h+\mu_h)^2x_2^* + x_1^*x_4^*\mu_h^2(\gamma_h+\mu_h+\mu_v))\beta_{vh} - x_5^*\mu_v^2(\gamma_h+\mu_h)^2],
\end{aligned}$$

and

$$\begin{aligned}
\beta_{hn}^{bt} =& \frac{1}{2}x_2^{*2}[(x_4^*-x_5^*)x_2^* + K(x_4^*-2x_5^*)]\gamma_h\beta_{vh}^2 + \beta_{vh}\left\{\left[\left(-\frac{1}{2}x_4^*\mu_h\right.\right.\right. \\
&\left.\left.\left. + \frac{1}{2}\mu_v(x_4^*-2x_5^*)\right)\gamma_h - \frac{1}{2}x_4^*\mu_h^2\right]x_2^{*2} - \left[\frac{1}{2}(x_4^*\mu_h + \mu_v(x_4^*-4x_5^*))K\gamma_h\right.
\end{aligned}$$

$$- \frac{1}{2}x_4^*(K - x_1^*)\mu_h^2\Big] x_2^* - Kx_1^*x_4^*\mu_h^2\Big\} - \left(K + \frac{1}{2}x_2^*\right) x_5^*\mu_v^2\gamma_h. \tag{4.9}$$

For the zero eigenvalue of J, there exists an eigenvector q, as shown in (4.7), and a corresponding generalized eigenvector q_g. For the transpose matrix of J, denoted as J^T, there exists an eigenvector p, as shown in (4.7), and a corresponding generalized eigenvector p_g, associated with the zero eigenvalue. We choose the generalized eigenvectors q_g and $\tilde{p}_g$ as follows:

$$q_g = \begin{bmatrix} q_{g1} \\ 1 \\ \dfrac{\gamma_h(\mu_h - 1)}{\mu_h^2} \\ -\dfrac{\beta_{vh}x_4^*(\beta_{vh}x_2^* + \mu_v - 1)}{(\beta_{vh}x_2^* + \mu_v)^2} \\ \dfrac{\beta_{vh}x_4^*(\beta_{vh}x_2^* + \mu_v - 1)}{(\beta_{vh}x_2^* + \mu_v)^2} \end{bmatrix}, \quad \tilde{p}_g = \begin{bmatrix} 1 \\ \tilde{p}_{g2} \\ 0 \\ \tilde{p}_{g4} \\ \tilde{p}_{g5} \end{bmatrix} \tag{4.10}$$

where

$$\begin{aligned}
q_{g1} =& \frac{1}{[\beta_h x_2^{*2} + (\beta_{hv}x_5^* + \mu_h)x_2^* + K(\beta_{hv}x_5^* + \mu_h)](\beta_{vh}x_2^* + \mu_v)^2(x_2^* + K)} \\
& \times \{-\beta_{vh}^2(\beta_h x_1^* + q_{g1})x_2^{*4} - 2\beta_{vh}(((\beta_h x_1^* + q_{g1})K + 1/2x_1^*x_4^*\beta_{hv})\beta_{vh} \\
& + \mu_v(\beta_h x_1^* + q_{g1}))x_2^{*3} + ((-2K\beta_{hv}x_1^*x_4^* - K^2 q_{g1})\beta_{vh}^2 + (-4\mu_v(\beta_h x_1^* + q_{g1})K \\
& - x_1^*x_4^*\beta_{hv}(\mu_v - 1))\beta_{vh} - \mu_v^2(\beta_h x_1^* + q_{g1}))x_2^{*2} - K(K\beta_{vh}^2 x_1^*x_4^*\beta_{hv} \\
& + (2K\mu_v q_{g1} + 2x_1^*x_4^*\beta_{hv}(\mu_v - 1))\beta_{vh} + 2\mu_v^2(\beta_h x_1^* + q_{g1}))x_2^* \\
& - (x_1^*x_4^*\beta_{hv}(\mu_v - 1)\beta_{vh} + \mu_v^2 q_{g1})K^2\}, \\
\tilde{p}_{g2} =& \frac{\beta_h x_2^{*2} + (\beta_{hv}x_5^* + \mu_h + 1)x_2^* + K(\beta_{hv}x_5^* + \mu_h + 1)}{K\beta_{hv}x_5^* + \beta_{hv}x_2^*x_5^* + \beta_h x_2^{*2}}, \\
\tilde{p}_{g4} =& \frac{\beta_{hv}\{[(\mu_h + 1)\mu_v - \mu_h]\beta_{vh}x_2^* + [(\mu_h + 1)\mu_v - 2\mu_h]\mu_v\}x_2^*x_1^*(x_2^* + K)\beta_{vh}}{(K\beta_{hv}x_5^* + \beta_{hv}x_2^*x_5^* + \beta_h x_2^{*2})\mu_v^2(\beta_{vh}x_2^* + \mu_v)^2}, \\
\tilde{p}_{g5} =& \frac{\beta_{hv}((\mu_h + 1)\mu_v - \mu_h)x_1^*(x_2^* + K)}{[\beta_h x_2^{*2} + \beta_{hv}x_5^*(x_2^* + K)]\mu_v^2}.
\end{aligned} \tag{4.11}$$

We take $n_2 =< p, q_g >$, where $<,>$ denotes the standard dot product, and have a normalized generalized eigenvector $p_g = \frac{\tilde{p}_g}{n_2}$. Moreover, the obtained eigenvectors and generalized eigenvectors satisfy that $Jq = 0$, $Jq_g = q$, $J^T p = 0$, $J^T p_g = p$, $< p_g, q >=< p, q_g >= 1$, and $< p_g, q_g >=< p, q >= 0$. Following the computation method in [22], we derive the normal form at the BT bifurcation as

$$\dot{u}_0 = u_1, \qquad \dot{u}_1 = a_{bt}u_0^2 + b_{bt}u_0u_1 + O(\| u \|^3), \tag{4.12}$$

where

$$
\begin{aligned}
a_{bt} &= \frac{1}{2}\sum_{i,j,k=1}^{5} p_i q_j q_k \frac{\partial^2 f_i(E^*, \beta_{hv}, \beta_h)}{\partial x_j \partial x_k} \\
&= \frac{a_{bt1}(x_2^* + 3K) + 3a_{bt2}K^2 x_2^* + a_{bt3}K^2}{n_2^2(x_2^* + K)^3}, \\
b_{bt} &= \sum_{i,j,k=1}^{5} p_{g_i} q_j q_k \frac{\partial^2 f_i(E^*, \beta_{hv}, \beta_h)}{\partial x_j \partial x_k} + \sum_{i,j,k=1}^{5} p_i q_j q_{g_k} \frac{\partial^2 f_i(E^*, \beta_{hv}, \beta_h)}{\partial x_j \partial x_k} \\
&= \frac{1}{n_2^2(x_2^* + K)^3}\{(3K + x_2^*)(b_{bt1} + 2b_{bt2} + b_{bt3} + b_{bt4})x_2^{*2} \\
&\quad + 3K^2 x_2^*(b_{bt1} + \frac{4}{3}b_{bt2} + b_{bt3} + \frac{2}{3}b_{bt4}) \\
&\quad + [(b_{bt1} + b_{bt3})K + 2x_1^*\beta_h(p_{g2} + p_2 - 2)]K^2\},
\end{aligned}
\tag{4.13}
$$

and

$$
\begin{aligned}
a_{bt1} =& [(p_2 - 1)(\beta_{hv}q_5 + \beta_h)q_1 - \beta_{vh}q_4(p_4 - p_5)]x_2^{*2}, \\
a_{bt2} =& (\beta_{hv}q_5 + \frac{2}{3}\beta_h)(p_2 - 1)q_1 - \beta_{vh}q_4(p_4 - p_5), \\
a_{bt3} =& (\beta_{hv}q_5(p_2 - 1)q_1 - \beta_{vh}q_4(p_4 - p_5))K + \beta_h x_1^*(p_2 - 1), \\
b_{bt1} =& [(2p_{g2} - 2)q_5 + q_{g5}(p_2 - 1)]\beta_{hv}q_1 + q_5 q_{g1}(p_2 - 1)\beta_{hv}, \\
b_{bt2} =& (p_{g2} + \frac{1}{2}p_2 - \frac{3}{2})\beta_h q_1, \\
b_{bt3} =& [(-2p_{g4} + 2p_{g5} - p_4 + p_5)q_4 - q_{g4}(p_4 - p_5)]\beta_{vh}, \\
b_{bt4} =& q_{g1}\beta_h(p_2 - 1).
\end{aligned}
\tag{4.14}
$$

Theorem 4.3. *The endemic equilibrium E^* of the ZIKV model* (2.1) *admits a double zero eigenvalue at $(\beta_{hv}, \beta_h) = (\beta_{hv}^{bt}, \beta_h^{bt})$ in* (4.9)*, and is locally topologically equivalent near the origin to*

$$
\dot{u}_0 = u_1, \qquad \dot{u}_1 = \mu_1 + \mu_2 u_0 + a_{bt}u_0^2 + b_{bt}u_0 u_1 + O(\| u \|^3)
$$

where μ_1 and μ_2 are the small perturbations.

Example for Bogdanov-Takens bifurcation. We choose β_{hv} and β_h as bifurcation parameters and set the other baseline parameter values as in Table 1. The model (2.1) undergoes a BT bifurcation on $E^* = (0.99456,\ 0.19809\times10^{-4},\ 0.54228\times 10^{-2},\ 0.99931,\ 0.69285\times10^{-3})$ at $(\beta_{hv},\ \beta_h) = (0.28675\times10^{-3},\ 0.94169)$. The three corresponding non-zero eigenvalues are -0.029963, -0.3653×10^{-4}, and -0.02. We choose an eigenvector and its generalized eigenvector for the zero eigenvalue for the corresponding Jacobian matrix as $q = (-0.36686\times10^{-4},\ 0.13353\times10^{-6},\ 0.36552\times 10^{-4},\ -0.46669\times10^{-5},\ 0.46669\times10^{-5})$ and $q_g = (1.0006,\ 0.13353\times10^{-6},\ -1.0006,\ 0.22852\times10^{-3},\ -0.22852\times10^{-3})$ and the corresponding adjoint eigenvector and its generalized eigenvector as $p = (1,\ 183.74,\ 0,\ 0.18054\times10^{-2},\ 2.6057)$ and $p_g = (15.591,\ 0.50053\times10^{7},\ 0,\ 49.269,\ 71242)$, then obtain the critical normal form (4.12) with coefficients $a_{bt} = -0.49317\times10^{-13}$ and $b_{bt} = 0.24565\times10^{-6}$. This BT bifurcation point shows in the 2-dimensional bifurcation diagram, Figure 1.

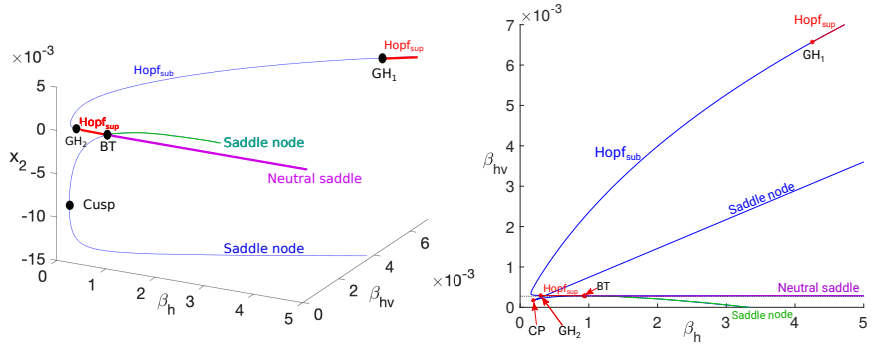

(a) 3-dimensional plot (b) 2-dimensional plot

Figure 1. Two-dimensional bifurcation diagrams.

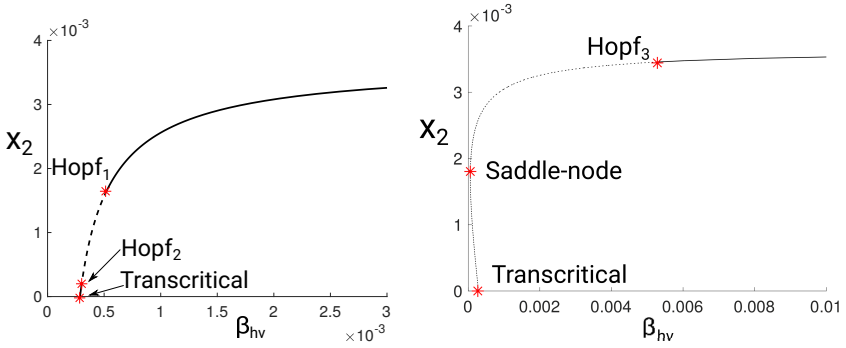

(a) $\beta_h = 0.2$ (b) $\beta_h = 3$

Figure 2. One-dimensional bifurcation diagrams.

4.4. Bifurcation diagrams

To demonstrate the influence of the vector and sexual routes on the dynamics of ZIKV transmission, we choose the vector-human and human-human transmission rates β_{hv} and β_h as bifurcation parameters and plot 2- and 1-dimensional bifurcation diagrams. Numerical bifurcation analysis demonstrates that saddle-node and Hopf bifurcation curves intersect at the Bogdanov-Takens (BT) bifurcation point. The BT bifurcation separates the saddle-node bifurcation curve into a part with positive x_2 (or I_h) value and another part with negative x_2 value, shown as green and blue saddle-node curves in Figure 1 (a). Considering the biological feasible region, we omit the dynamics in the x_2 negative section. That is, the blue saddle-node bifurcation curve in Figure 1 (a) and (b). The BT bifurcation delimits the Hopf curve into a neutral saddle section and a supercritical Hopf bifurcation section. The later section becomes a subcritical bifurcation section when it passes through a general Hopf bifurcation, GH_2, then eventually turns back to a supercritical Hopf bifurcation section when it passes through another general Hopf bifurcation, GH_1. Here, GH_1 happens at $E^* = (0.039535, 0.34958 \times 10^{-2}, 0.024399, 0.89098, 0.10901)$ and $(\beta_{hv}, \beta_h) = (0.65703 \times 10^{-2}, 4.2517)$ and

GH_2 happens at $E^* = (0.97551, 0.89131 \times 10^{-4}, 0.024399, 0.99689, 0.31098 \times 10^{-2})$ and $(\beta_{hv}, \beta_h) = (0.29233 \times 10^{-3}, 0.29887)$. A cusp bifurcation happens out of biological feasible region at $E^* = (1.00006, -0.241515 \times 10^{-6}, -0.661131 \times 10^{-4}, 1.000008, 0.845297 \times 10^{-5})$ and $(\beta_{hv}, \beta_h) = (0.29233 \times 10^{-3}, 0.29887)$. Choosing $\beta_h = 0.2$ and $\beta_h = 3$, one-dimensional bifurcation diagrams in Figure 2 demonstrate forward and backward bifurcations. Moreover, three subcritical Hopf bifurcation occur at $E^*_{H1} = (0.553880, 0.16237 \times 10^{-2}, 0.44449, 0.94622, 0.053775)$ with $\beta_{hv} = 0.51463 \times 10^{-3}$ and $l_0 = 2.6804 \times 10^3$ and $E^*_{H2} = (0.94519, 0.19947 \times 10^{-3}, 0.054604, 0.99307, 0.69331 \times 10^{-2}$ with $\beta_{hv} = 0.301679 \times 10^{-3}$ and $l_0 = 8.1534 \times 10^4$ for $\beta_h = 0.2$, and $E^*_{H3} = (0.050538, 0.345576 \times 10^{-2}, 0.946006, 0.892099, 0.107901)$ with $\beta_{hv} = 0.52663 \times 10^{-2}$ with $l_0 = 1.4681 \times 10^4$ for $\beta_h = 3$. Here, l_0 denotes the first Lyapunov coefficient.

5. Simulated low-level ZIKV transmission and outbreaks.

The occurrence of Hopf bifurcation provides an oscillation source, which potentially induces flareups after a long period of silence for periodic solutions [41, 43]. For the two cases $\beta_h = 0.2$ and $\beta_h = 3$ in Figure 2, model (2.1) admits subcritical Hopf bifurcations. Low-level ZIKV transmission and uniform outbreaks with long periods are simulated due to the spread of oscillations from the Hopf bifurcations in Figure 3.

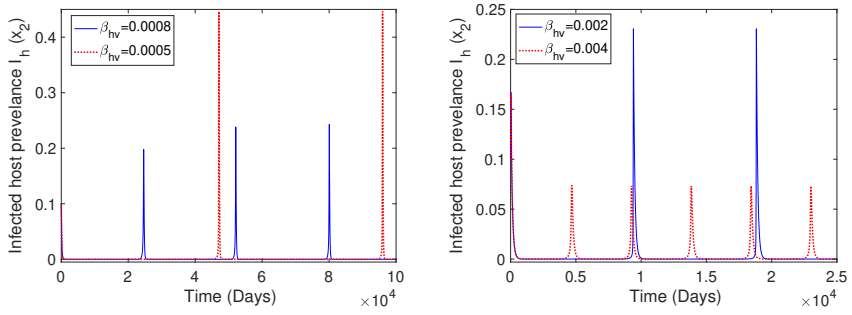

(a) $\beta_h = 0.2$ (b) $\beta_h = 3$

Figure 3. Simulated low-level ZIKV transmission with uniform outbreaks

Environmental conditions affect the vector-human transmission in a random manner. To study this influence, we consider stochastic influence on the vector-human transmission route, and formulate an Itô stochastic differential equation of $\beta_{hv}(t)$ by a mean reverting stochastic process [3, 42] as

$$d\beta_{hv}(t) = r(\beta_{hv_0} - \beta_{hv}(t))dt + \sigma\beta_{hv}(t)dW(t). \tag{5.1}$$

Note that, here, $r > 0$ denotes the return rate of β_{hv} to its mean rate β_{hv_0}, σ is the deviation from the mean during the return process and $\sigma > 0$, and W is the standard Wiener process. We require an adequately large the return rate r, such as $2r > \sigma^2$, to guarantee that $\lim_{x\to\infty} E(\beta_{hv}(t)|\beta_{hv}(0)) = \beta_{hv_0}$ and

$\lim_{x\to\infty} Var(\beta_{hv}(t)|\beta_{hv}(0)) = \dfrac{\sigma^2\beta_{hv_0}^2}{2r-\sigma^2}$ are finite. Here, β_{hv} proceed towards a steady state level which has a constant variance. Taking $\beta_{hv_0} = 0.003$, $r = 1$, $\sigma = 0.8$, an example sample paths of infected host prevalence I_h is plotted in Figure 4. The simulation shows outbreaks with varying amplitudes and periods.

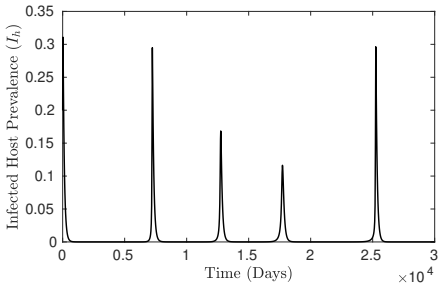

Figure 4. Low-level ZIKV transmission with varied outbreak periods and amplitude.

6. Disease control measures

To minimize the human infection rate due to ZIKV, it is crucial to determine the factors that influence the transmission of ZIKV. Here, by conducting a sensitivity analysis, we investigate the parameters that highly impact R_0 and I_h at endemic equilibrium E^* and discuss the disease control strategies. Sensitivity indices can be recognized as a measure of relative change in a variable while a parameter varies. The relative variation of a variable to the relative change of a parameter is called the normalized forward sensitivity index, which is calculated for a variable with respect to a model parameter.

6.1. Sensitivity indices of R_0

We conduct a sensitivity analysis on the basic reproduction number to find out the parameters that significantly impact the basic reproduction number R_0. The normalized forward sensitivity index of R_0 [10] is given below by the equation $\gamma_p^{R_0} = \frac{\partial R_0}{\partial p} \times \frac{p}{R_0}$ where p is a model parameter. The higher values in its magnitude show more sensitivity to the R_0. The positive or negative signs indicate whether the R_0 has an increase or decrease when the parameter p increases. Also, the indices computations are for all parameters which could be influenced by public health attempts.

We calculated sensitivity indices of R_0 with respect to the parameters, which can be influenced by public health efforts. Since the $\gamma_V^{R_0} = \gamma_{\beta_{hv}}^{R_0} = \gamma_{\beta_{vh}}^{R_0} = 0.5$, increasing (decreasing) the vectors' recruitment rate V, the contact rate between infected vectors and susceptible human β_{hv}, and the contact rate between infected human and susceptible vectors β_{vh} by 10% will increase (decrease) the R_0 by 5%. Moreover, since $\gamma_{\mu_v}^{R_0} = -1$, increasing (decreasing) the death rate of vectors μ_v by 10% will decrease (increase) R_0 by 10%. Additionally, since $\gamma_{\gamma_h}^{R_0} = -0.1667$ increasing (decreasing) of the recovery rate of infected human γ_h by 10% will decrease

(increase) R_0 by 16.67%. We note that sexual transmission rate β_h does not affect the basic reproduction number. However, varying sexual transmission rates result in complex disease dynamics such as Hopf and backward bifurcations, as shown in Figure 1.

6.2. Sensitivity indices of E^*

According to the study [10], we can calculate the sensitivity indices of the endemic equilibrium E^* numerically using the parameter values given in Table 1 and there exists the unique positive endemic equilibrium at $E^* = (x_i^*)_{i=1...5} = (S_h^*, I_h^*, R_h^*, S_v^*, I_v^*) = (4.6131 \times 10^{-4}, 3.6380 \times 10^{-3}, 9.9590 \times 10^{-1}, 8.8705 \times 10^{-1}, 1.1295 \times 10^{-1})$. Note that, we cannot derive an analytical expression for sensitivity indices of state variables at E^* since we do not have an explicit formula for endemic equilibrium. The sensitivity index of the state variable at the endemic equilibrium x_i, to the parameter p_j, is given by $\gamma_{p_j}^{x_i} = \frac{\partial x_i}{\partial p_j} \times \frac{p_j}{x_i}$, where the five state variables at the endemic equilibrium point $(S_h^*, ..., I_v^*)$ are given as $(x_1, ..., x_5)$ and the nine parameters $(H, V, ..., K)$ are given as $(p_1, p_2, ..., p_9)$ for $i = 1, ..., 5$ and $j = 1, ..., 9$. It measures the relative change in solution x_i to the variations in the parameter p_j. The five equilibrium equations in the model (2.1) can be written as $f_i(x_1, ..., x_5; p_1, ..., p_9) = 0$ for $i = 1, ..., 5$. Then we can calculate $\partial x_i/\partial p_j$ by solving the equation $Jz^{(j)} = b^{(j)}$ for $j = 1, ..., 9$ where J is the (5×5) Jacobian of the ZIKV model (2.1) with $J_{ki} = \partial f_k/\partial x_i$ and $1 \leq k \leq 5$; $z^{(j)}$ is the unknown (5×1) vector where the $\partial x_i/\partial p_j$ is the i^{th} term of the vector $z^{(j)}$. Also the (5×1) vector $b^{(j)}$ has the k^{th} term given as $-\partial f_k/\partial p_j$. The matrix J and vector $b^{(j)}$ are known because we can assess the Jacobian at the calculated endemic equilibrium and for the given parameter values in Table 1. In similar manner, we can evaluate the vector $b^{(j)}$ by calculating the derivative $-\partial f_k/\partial p_j$.

The sensitivity indices are numerically calculated for the state variable of interest, I_h, at endemic equilibrium E^* as $\gamma_{\gamma_h}^{x_2} = -0.9967$ and $\gamma_{\mu_v}^{x_2}$, $\gamma_V^{x_2}$, $\gamma_{\beta_{hv}}^{x_2}$, $\gamma_{\beta_{vh}}^{x_2}$, and $\gamma_{\beta_h}^{x_2}$ are in the order of $O(-4)$.

Therefore, the most sensitive parameter for I_h is γ_h.

That is, increasing γ_h by 10% would reduce the infected host prevalence by 9.967%. Sensitivity analysis here suggests that prevention programs should mainly focus their attention on bringing down the mosquito life span and boost human immunity to reduce the ZIKV infected prevalence.

6.3. Target reproduction number $\mathcal{T}_S$

It is well known that the basic reproduction number R_0 is a crucial threshold quantity when determining whether an infectious disease will decline or die out. However, this quantity is applied to the entire susceptible population. Target reproduction numbers are helpful when we establish disease control strategies by aiming at different transmission types in a disease model. According to [30] and [33], we can calculate the target reproduction number related to ZIKV transmission routes. Since the target reproduction number is based on entries in the next-generation matrix, we note that no entries are related to the sexual transmission rate β_h. Hence, we can only compute the target reproduction number related to the mosquito transmission route.

Consider the next-generation matrix for the model (2.1),

$$FV^{-1} = K = \begin{bmatrix} K_{11} & K_{12} \\ K_{21} & K_{22} \end{bmatrix} = \begin{bmatrix} 0 & \frac{H\beta_{hv}}{\mu_h\mu_v} \\ \frac{V\beta_{vh}}{(\gamma_h+\mu_h)\mu_v} & \end{bmatrix}$$

and according to [33], we choose the target set as $S = \{(1,2)\}$ which is associated with control of vector to human transmission. We take $S_1 = \{1\}$ and $S_2 = \{2\}$ and write the target reproduction number

$$\mathcal{T}_S = \rho\left(\frac{E_{S_1}P_{S_1}KP_{S_2}E_{S_1}}{I - K + P_{S_1}KP_{S_2}}\right), \tag{6.1}$$

where, $E_{S_1} = P_{S_1} = \begin{bmatrix} 1 & 0 \\ 0 & 0 \end{bmatrix}$ and $P_{S_2} = \begin{bmatrix} 0 & 0 \\ 0 & 1 \end{bmatrix}$. Hence, we have,

$$\mathcal{T}_S = K_{12}K_{21} = R_0^2.$$

Thus, if a fraction of more than $1 - \frac{1}{\mathcal{T}_S} = \frac{R_0^2-1}{R_0^2}$ of vector to human transmitted infections can be prevented, then ZIKV can be eradicated. This is potentially achieved by reducing mosquito lifespan, reducing mosquito bites (using insect repellents, wearing clothes that cover arms and legs, mosquito netting [9]) and other control methods such as releasing Wolbachia infected mosquitoes [20].

7. Conclusion

A large outbreak of ZIKV took place in 2016 in the Americas, with serious intimation for public health in the region. The World Health Organization then asserted that the emergence of ZIKV as a public health emergency due to the neurological disorders and severe birth complications associated with the infection, such as microcephaly. Although the transmission of ZIKV has reduced since then, ZIKV remains endemic in many regions of the world. However, understanding future disease incidences is limited due to the lack of detection and reporting of ZIKV infection cases, especially in areas with the low-level transmission. A recent study in Lancet [31] provides evidence of the long-term circulation of ZIKV for at least sixteen years and its threat to public health in Thailand. They highlight that poor understanding of the low and long-term transmission of ZIKV has led the virus to maintain itself and circulate silently. The poor understanding of long-term transmission is not surprising due to the misdiagnosis of symptoms of ZIKV as symptoms of dengue or chikungunya. According to the studies, more than 280 microcephaly cases were reported during the period 2016-2018, and mothers of these newborns were not previously identified as ZIKV infected. Since ZIKV infected pregnant women can pass the virus to her fetus, the study [31] warns that there will be severe complications. The findings of the study suggest that ZIKV transmission in the long term can be transited into an endemic transmission, and outbreaks of the disease might happen in future years. Therefore, the study alarms the necessity for developing effective prevention and surveillance programs to understand the spread of the disease and the occurrence of ZIKV related health outcomes. Hence, the mechanism behind low

persistent and re-emerging ZIKV with short epidemic duration and long lead time should be thoroughly analyzed.

Alarmed by the long-term circulation of ZIKV in Thailand [31], we formulate a ZIKV transmission model to predict future outbreaks and disease control. Our model successfully simulates the low-level persistent ZIKV transmission with short periods of outbreaks. Due to the additional human-human sexual transmission route, modeled by a Poisson point process, backward bifurcation occurs in our model even though the disease related deaths are assumed to be zero. It further induces the occurrence of Hopf bifurcation, which is the source of the oscillations, with long periods of quiet episodes and sharp outbreaks. Furthermore, we find that the varying amplitudes and periods of outbreaks can be caused by stochastic influences on the sexual transmission rate.

Our study investigated the stability of the disease-free equilibrium and presented several control strategies. If the basic reproduction number $R_0 < 1$, ZIKV dies out; otherwise, ZIKV persists. It is noteworthy that sexual transmission alone cannot drive the ZIKV epidemic, as the basic reproduction number does not depend on the sexual transmission rate. By considering that the impact of sexual transmission on disease dynamics is negligible, by setting $\beta_h = 0$, we observed that $R_0 < 1$ is the sufficient and necessary condition for complete disease eradication. However, when the sexual transmission route is present, the disease eradication becomes more complicated, and the basic reproduction number is less than unity is no more sufficient. Not only that, but it also leads to multi-annual disease outbreaks, so the public health policymakers should pay attention to the control of the potential future emergence of ZIKV. The reason behind the complex consequences of sexual transmission is the slow timescale associated with virus clearance on semen. Even though the virus gets cleared from the blood within weeks, the virus in semen stays for several months after infection. Then the virus can circulate at low levels until favorable environmental conditions cause an outbreak.

The sensitivity analysis for the R_0 concludes that the increase in natural death rate of mosquitoes will decrease the basic reproduction number, and it has the largest impact on R_0. It suggests that prevention programs should mainly focus on reducing the mosquito life span to reduce the infection of ZIKV. Spraying adulticides and larvicides will reduce the mosquitoes' life span, and mosquito control programs may use aerial and truck spraying to control the mosquitoes in a large area. Moreover, releasing sterile mosquitoes is a smart way to control the virus carrying mosquito population. An increase in human recovery rate has the largest effect on decreasing human host prevalence at the endemic equilibrium. Even though ZIKV has no specific antiviral treatment, resting, increasing fluid intake, and taking medication would help treat the symptoms. However, local governments and mosquito prevention programs should plan to conduct researches on specific antiviral treatments for ZIKV. Furthermore, sensitivity analysis of R_0 and sensitivity analysis of I_h at E^* showed that reducing the recruitment rate of vectors and mosquito biting rates β_{hv} and β_{vh} will reduce the R_0 and disease host prevalence. So, the ZIKV prevention programs may pay their attention to decreasing mosquito recruitment by stopping laying eggs in or near water, removing standing water, covering fountains, septic tanks, pools with covers etc. Additionally, using insect repellents, wearing clothes covering arms and legs, and mosquito netting may reduce the humans getting infected by a mosquito biting [9]. More importantly, in this paper, we focused not only on mosquito transmission but sexual transmission also. For

the basic reproduction number, the effect of sexual transmission is zero. However, a decrease in sexual transmission rate decreases the infected host population. Conducting awareness programs on protection during sex will help decrease the sexual transmission rate. Even though, note that the influence of sexual transmission rate on the growth of disease is very low when it is compared to the other parameters, both sexual and vector transmission must be controlled for the better control of ZIKV epidemic.

While our model was constructed based on the results shown in [31], we must note that the data set used in that study was not readily available at the time of the writing and submission of this paper. As such, we cannot directly verify how well the behavior exhibited by this model matches real-world observations for the region and time studied in that manuscript. Thus, to more thoroughly assess the practical implications of the dynamics studied in this paper, one key area of future work is to fit the data, should it become available, to the model.

References

[1] A. T. Aborode, M. Sukaina, H. Kumar et al., *Zika virus endemic challenges during COVID-19 pandemic in Africa*, Tropical Medicine and Health, 2021, 49(1), 1–4.

[2] F. Agusto, S. Bewick and W. Fagan, *Mathematical model for Zika virus dynamics with sexual transmission route*, Ecological Complexity, 2017, 29, 61–81.

[3] L. Allen, *An introduction to stochastic processes with applications to biology*, CRC Press, Boca Raton, Fl., 2010.

[4] D. Baud, D. J. Gubler, B. Schaub et al., *An update on Zika virus infection*, The Lancet, 2017, 390(10107), 2099–2109.

[5] S. Bilal and E. Michael, *Effects of complexity and seasonality on backward bifurcation in vector–host models*, Royal Society Open Science, 2018, 5(2), 171971.

[6] S. K. Biswas, U. Ghosh and S. Sarkar, *Mathematical model of Zika virus dynamics with vector control and sensitivity analysis*, Infectious Disease Modelling, 2020, 5, 23–41.

[7] V. M. Cao Lormeau, A. Blake, S. Mons et al., *Guillain-Barré syndrome outbreak associated with Zika virus infection in French Polynesia: a case-control study*, The Lancet, 2016, 387(10027), 1531–1539.

[8] V. M. Cao Lormeau and D. Musso, *Emerging arboviruses in the Pacific*, The Lancet, 2014, 384(9954), 1571–1572.

[9] CDC, *Mosquito control in a community*, Centers for Disease Control and Prevention, 2020.

[10] N. Chitnis, J. M. Hyman and J. M. Cushing, *Determining important parameters in the spread of malaria through the sensitivity analysis of a mathematical model*, Bulletin of Mathematical Biology, 2008, 70(5), 1272.

[11] D. A. Cummings, S. Iamsirithaworn, J. T. Lessler et al., *The impact of the demographic transition on dengue in Thailand: insights from a statistical analysis and mathematical modeling*, PLoS Medicine, 2009, 6(9), e1000139.

[12] M. R. Duffy, T.-H. Chen, W. T. Hancock et al., *Zika virus outbreak on Yap Island, federated states of Micronesia*, New England Journal of Medicine, 2009, 360(24), 2536–2543.

[13] A. Enfissi, J. Codrington, J. Roosblad et al., *Zika virus genome from the Americas*, The Lancet, 2016, 387(10015), 227–228.

[14] N. M. Ferguson, Z. M. Cucunubá, I. Dorigatti et al., *Countering the Zika epidemic in Latin America*, Science, 2016, 353(6297), 353–354.

[15] D. Gao, Y. Lou, D. He et al., *Prevention and control of Zika as a mosquito-borne and sexually transmitted disease: a mathematical modeling analysis*, Scientific Reports, 2016, 6(1), 28070.

[16] N. K. Goswami, A. K. Srivastav, M. Ghosh and B. Shanmukha, *Mathematical modeling of Zika virus disease with nonlinear incidence and optimal control*, in *Journal of Physics: Conference Series*, 1000, IOP Publishing, 2018, 012114.

[17] A. B. Gumel, *Causes of backward bifurcations in some epidemiological models*, Journal of Mathematical Analysis and Applications, 2012, 395(1), 355–365.

[18] J. Ikejezie, C. N. Shapiro, J. Kim et al., *Zika virus transmission—region of the Americas, May 15, 2015–December 15, 2016*, MMWR. Morbidity and Mortality Weekly Report, 2017, 66(12), 329.

[19] M. Kama, M. Aubry, T. Naivalu et al., *Sustained low-level transmission of Zika and chikungunya viruses after emergence in the Fiji Islands*, Emerging Infectious Diseases, 2019, 25(8), 1535.

[20] J. Kamtchum Tatuene, B. L. Makepeace, L. Benjamin et al., *The potential role of Wolbachia in controlling the transmission of emerging human arboviral infections*, Current Opinion in Infectious Diseases, 2017, 30(1), 108.

[21] W. O. Kermack and A. G. McKendrick, *A contribution to the mathematical theory of epidemics*, Proceedings of the Royal Society of London. Series A, Containing Papers of a Mathematical and Physical Character, 1927, 115(772), 700–721.

[22] Y. A. Kuznetsov, *Elements of applied bifurcation theory*, 112, Springer Science & Business Media, 2013.

[23] J. Lessler, L. H. Chaisson, L. M. Kucirka et al., *Assessing the global threat from Zika virus*, Science, 2016, 353(6300), aaf8160.

[24] G. H. Li and Y. X. Zhang, *Dynamic behaviors of a modified SIR model in epidemic diseases using nonlinear incidence and recovery rates*, PLoS One, 2017, 12(4), e0175789.

[25] M. Lozier, L. Adams, M. F. Febo et al., *Incidence of Zika virus disease by age and sex—Puerto Rico, November 1, 2015–October 20, 2016*, Morbidity and Mortality Weekly Report, 2016, 65(44), 1219–1223.

[26] J. Mlakar, M. Korva, N. Tul et al., *Zika virus associated with microcephaly*, New England Journal of Medicine, 2016, 374(10), 951–958.

[27] C. Nutt and P. Adams, *Zika in Africa—the invisible epidemic?*, The Lancet, 2017, 389(10079), 1595–1596.

[28] Á. G. Pérez, E. Avila-Vales and G. E. García-Almeida, *Bifurcation analysis of an SIR model with logistic growth, nonlinear incidence, and saturated treatment*, Complexity, 2019. DOI: 10.1155/2019/9876013.

[29] T. C. Pierson and M. S. Diamond, *The emergence of Zika virus and its new clinical syndromes*, Nature, 2018, 560(7720), 573–581.

[30] M. Roberts and J. Heesterbeek, *A new method for estimating the effort required to control an infectious disease*, Proceedings of the Royal Society of London. Series B: Biological Sciences, 2003, 270(1522), 1359–1364.

[31] K. Ruchusatsawat, P. Wongjaroen, A. Posanacharoen et al., *Long-term circulation of Zika virus in Thailand: an observational study*, The Lancet Infectious Diseases, 2019, 19(4), 439–446.

[32] C. Saad-Roy, J. Ma and P. van den Driessche, *The effect of sexual transmission on Zika virus dynamics*, Journal of Mathematical Biology, 2018, 77(6-7), 1917–1941.

[33] Z. Shuai, J. Heesterbeek and P. van Den Driessche, *Extending the type reproduction number to infectious disease control targeting contacts between types*, Journal of Mathematical Biology, 2013, 67(5), 1067–1082.

[34] Z. Shuai and P. van den Driessche, *Global stability of infectious disease models using Lyapunov functions*, SIAM Journal on Applied Mathematics, 2013, 73(4), 1513–1532.

[35] V. Sikka, V. K. Chattu, R. K. Popli et al., *The emergence of Zika virus as a global health security threat: a review and a consensus statement of the INDUSEM Joint Working Group (JWG)*, Journal of Global Infectious Diseases, 2016, 8(1), 3.

[36] P. Suparit, A. Wiratsudakul and C. Modchang, *A mathematical model for Zika virus transmission dynamics with a time-dependent mosquito biting rate*, Theoretical Biology and Medical Modelling, 2018, 15(1), 11.

[37] D. Taylor, *Mathematical model of Zika virus transmission and control measures*, The North Carolina Journal of Mathematics and Statistics, 2021, 7(1), 1–12.

[38] H. R. Thieme, *Mathematics in population biology*, 12, Princeton University Press, 2018.

[39] P. van den Driessche and J. Watmough, *Reproduction numbers and subthreshold endemic equilibria for compartmental models of disease transmission*, Mathematical Biosciences, 2002, 180(1), 29 – 48.

[40] J. Wang, S. Liu, B. Zheng and Y. Takeuchi, *Qualitative and bifurcation analysis using an SIR model with a saturated treatment function*, Mathematical and Computer Modelling, 2012, 55(3-4), 710–722.

[41] W. Zhang, *Modeling and analysis of the multiannual Cholera outbreaks with host-pathogen encounters*, International Journal of Bifurcation and Chaos, 2020, 30(08), 2050120.

[42] W. Zhang, *Deterministic and stochastic in-host tuberculosis models for bacterium-directed and host-directed therapy combination*, Mathematical Medicine and Biology: A Journal of the IMA, 2022, 39(2), 126–155.

[43] W. Zhang and P. Yu, *Revealing the role of the effector-regulatory T cell loop on autoimmune disease symptoms via nonlinear analysis*, Communications in Nonlinear Science and Numerical Simulation, 2021, 93, 105529.